



## Clinical significance of three-dimensional power Doppler combined with two-dimensional Doppler ultrasonography for evaluating fetal growth restriction

Hui Fan, Lili Li & Changfu Hao

To cite this article: Hui Fan, Lili Li & Changfu Hao (2024) Clinical significance of three-dimensional power Doppler combined with two-dimensional Doppler ultrasonography for evaluating fetal growth restriction, The Journal of Maternal-Fetal & Neonatal Medicine, 37:1, 2322610, DOI: [10.1080/14767058.2024.2322610](https://doi.org/10.1080/14767058.2024.2322610)

To link to this article: <https://doi.org/10.1080/14767058.2024.2322610>



© 2024 The Author(s). Published by Informa UK Limited, trading as Taylor & Francis Group



Published online: 28 Feb 2024.



Submit your article to this journal [↗](#)



Article views: 900



View related articles [↗](#)



View Crossmark data [↗](#)

# Clinical significance of three-dimensional power Doppler combined with two-dimensional Doppler ultrasonography for evaluating fetal growth restriction

Hui Fan<sup>a</sup>, Lili Li<sup>a</sup>  and Changfu Hao<sup>b</sup>

<sup>a</sup>Department of Ultrasound, The Third Affiliated Hospital of Zhengzhou University, Henan, China; <sup>b</sup>Department of Child and Adolescence Health, College of Public Health, Zhengzhou University, Henan, China

## ABSTRACT

**Objectives:** To assess the predictive accuracy of three-dimensional (3D) power Doppler combined with two-dimensional (2D) Doppler ultrasonography in detecting fetal growth restriction (FGR).

**Methods:** The study was conducted on singleton pregnancies presenting for growth ultrasound examinations between 20 and 40 weeks of gestation. 63 patients with FGR were enrolled and matched 1:1.8 for gestational age with normal fetuses. Both groups were further divided into subgroups, with 32 weeks as the threshold—early-onset and late-onset FGR groups, and corresponding control groups. Conventional 2D Doppler parameters and standardized 3D power Doppler measurements of the placenta, including vascularization index (VI), flow index (FI), and vascularization-flow index (VFI) were obtained for each patient.

**Results:** (1) The average gestational weeks of delivery and birth weight of newborns in early-onset and late-onset FGR case groups were lower than those in control groups, while the incidence of placenta previa and adverse pregnancy outcomes were higher than those in control groups. (2) The biparietal diameter, head circumference, abdominal circumference, femur length, estimated fetal weight, middle cerebral artery systolic/diastolic velocity ratio (S/D), pulsatility index (PI), resistance index (RI), and placental blood perfusion indices of vascular index (VI), flow index (FI), vascular flow index (VFI), and cerebro-placental ratio (CPR) of the early-onset and late-onset FGR case groups were all lower than those of the control group. Moreover, the S/D, PI, and RI of the umbilical and uterine arteries were higher than those of the corresponding control group. (3) For early-onset FGR, the area under the curve (AUC) of the umbilical artery PI was the largest (0.861), exhibiting the highest predictive value. When combined with the placental blood perfusion index, the AUC was 0.789. For late-onset FGR, the AUC of the CPR was 0.861. After integrating the placental blood perfusion index, the AUC increased to 0.877. The positive likelihood ratio (PLR) of combined 2D Doppler indexes (21.938) and negative likelihood ratio (NLR) of VFI (0.565) were the highest in the early-onset FGR group. The PLR of combined 3D Doppler indexes (8.536) and NLR of VFI (0.557) were the highest in the late-onset FGR group.

**Conclusions:** The combination of 3D Doppler indices with 2D Doppler ultrasonography demonstrated superior predictive value in diagnosing late-onset FGR compared to other conventional indicators. The 3D Dower index, VFI, has a good true-negative predictive value for both early- and late-onset FGR.

## ARTICLE HISTORY

Received 22 November 2023

Revised 6 February 2024

Accepted 19 February 2024

## KEYWORDS

Intrauterine growth restriction;  
three-dimensional power Doppler ultrasound;  
ultrasonic examination;  
Doppler

## Introduction

Fetal growth restriction (FGR) is characterized by a fetal abdominal circumference (AC) or estimated fetal weight (EFW) below the 10th percentile of the normal standard for gestational age (GA) [1]. This condition occurs when a fetus has not attained its full growth potential due to various influencing factors such as

the placenta, maternal health, fetal development, and genetics. FGR can be categorized into early-onset (< 32 weeks) and late-onset ( $\geq$  32 weeks) based on the timing of onset [2]. FGR may result in fetal hypoxia and growth impairment due to hindered transfer of oxygen and nutrients to the fetus, potentially leading to premature delivery, low birth weight, neonatal asphyxia, neonatal polycythemia, meconium aspiration

**CONTACT** Hui Fan  [fanhuifh@yeah.net](mailto:fanhuifh@yeah.net)  Department of Ultrasound, The Third Affiliated Hospital of Zhengzhou University, Henan 450052, China

© 2024 The Author(s). Published by Informa UK Limited, trading as Taylor & Francis Group

This is an Open Access article distributed under the terms of the Creative Commons Attribution License (<http://creativecommons.org/licenses/by/4.0/>), which permits unrestricted use, distribution, and reproduction in any medium, provided the original work is properly cited. The terms on which this article has been published allow the posting of the Accepted Manuscript in a repository by the author(s) or with their consent.

syndrome, and stillbirth. Additionally, the long-term metabolic and neurobehavioral development of affected children and adolescents may be impacted. At present, effectively identifying and preventing FGR remains a challenge.

2D Doppler ultrasonography of major fetal circulation sites is commonly employed to evaluate placental vascular function in FGR and estimate the hemodynamic condition of growth-restricted fetuses [3]. With advancements in ultrasound technology, 3D power Doppler ultrasound can be utilized to monitor blood flow in placental volume samples and directly estimate placental perfusion. This method offers benefits such as sensitivity to low-speed blood flow and independence from angle dependency [4]. In recent years, numerous studies have explored the value of blood-flow spectrum monitoring for FGR; however, few investigations have combined hemodynamic assessments with placental blood perfusion evaluations.

The objective of this study was to explore the clinical utility of 3D power Doppler ultrasonography combined with 2D Doppler in evaluating FGR and compare the findings with those obtained using conventional 2D Doppler analysis alone.

## Materials and methods

### Patients and study design

This study involved pregnant women with suspected FGR from The Third Affiliated Hospital of Zhengzhou University between January 2020 and December 2021. Fetuses diagnosed with FGR were defined according to the consensus [5]. Inclusion criteria consisted of apparently healthy women with singleton pregnancies between 20 and 40 weeks of gestation and accurate pregnancy dating based on first-trimester ultrasound scans. Exclusion criteria included multiple gestations, major congenital anomalies, chromosomal abnormalities, umbilical cord/placental abnormalities such as placenta previa, posterior wall placenta, velamentous placenta, or placental chorioangioma, maternal congenital uterine malformations, smoking during pregnancy, and exposure history to toxic or radioactive substances. Finally, 63 patients with FGR between 20 and 40 weeks of gestation were enrolled and matched 1:1.8 for gestational age with normal fetuses. Both groups were further divided into subgroups, with 32 weeks as the threshold—early-onset and late-onset FGR groups, and corresponding control groups.

Data collected from maternal medical records included the age of pregnant women, gestational age (GA) at inclusion, fetal biometry data (biparietal

diameter-BPD, head circumference-HC, abdominal circumference-AC, femur length-FL), 2D Doppler data of the umbilical artery (UA), middle cerebral artery (MCA), and uterine arteries (UtA), as well as 3D power Doppler data. After delivery, information such as gestational age at delivery, birth weight, gender, delivery mode, and newborn outcomes were collected. A composite fetal/neonatal adverse outcome was defined as one or more events of intrauterine death, neonatal death, preterm delivery, a 5-min Apgar score <7, respiratory distress syndrome (NRDS), or low birth weight infants (LBWI).

All participating women consented to undergo the complete ultrasound examination after being thoroughly informed about the study protocol and the technique. This study protocol was approved by the local institutional ethical committee. Each pregnant woman who participated in the study signed a written informed consent form.

### Acquisition of 2D doppler velocity waveforms

All measurements were performed using a Voluson E8 (GE Healthcare) ultrasound machine, equipped with a 3.0–5.0 MHz in the middle and late pregnancy examination mode. Recordings used for measurements were obtained when the fetus showed no body movements, and the pregnant woman was instructed to hold her breath when necessary. All values were averaged over at least 3 consecutive measurements. The ideal measurement angle occurred when the sound beam and blood flow were completely parallel. During the measurement, 3–10 continuous waveforms were recorded. The free UA was selected for measurement. For the MCA, magnification was employed after sectioning the cerebral axis, which included the thalamus and the greater wing of the sphenoid bone. Color Doppler flow imaging (CDFI) was used to display the Willis ring and the proximal MCA. The pulse-Doppler sampling frame was placed in the proximal third of the MCA, near the origin of the internal carotid artery (the further it was from the origin of the internal carotid artery, the lower the systolic flow velocity). Care was taken to avoid unnecessary pressure on the fetal head during the measurement.

For the UtA, the probe was placed in the lower abdomen for transabdominal ultrasound measurements, and CDFI was employed to locate the intersection of the UtA with the external iliac artery to identify the UtA. The sample volume of the UtA was placed 1 cm downstream of the intersection. In a small number of cases, the branch of the UtA was located before the intersection of the external iliac artery; thus, the sampling volume was placed before the bifurcation of

the UtA. After obtaining a satisfactory stable spectral image, a stop frame and automatic envelope function were initiated to measure the following blood flow parameters: pulsatility index (PI) of the maternal UtA, fetal MCA, and fetal UA, resistance index (RI), systolic/diastolic velocity ratio (S/D), and cerebroplacental ratio (CPR; the ratio of MCA PI to UA PI).

### Acquisition of 3D placental vascular indices

Placental blood flow perfusion was observed by trained obstetric sonographers using preestablished instrument power settings on Voluson E8 ultrasound machines equipped with 3.0-5.0MHz transducers (GE Healthcare; angio mode, cent; smooth, 4/5; FRQ, low; quality, 16; density, 6; enhance, 16; balance, GO150; filter, 2; actual power, 2dB; and pulse repetition frequency, 0.9). The power Doppler button was activated to initiate imaging, and an appropriate sample volume was chosen, encompassing placental tissue from the placental basement membrane surface to the fetal surface where the umbilical cord connected to the placenta. Instrument parameters were adjusted to optimize the display of low-velocity blood flow in the placenta, clearly illustrating the complete vascular tree from the base to the chorionic plate (including small villus vessels in the placenta as much as possible). The 3D button was pressed, and the 3D power Doppler condition was selected for image acquisition. During image acquisition, the probe remained stable. Participants were instructed to keep still and to hold their breath if necessary. After data collection, volume analysis data were selected using the VOCAL automatic mode. The rotation angle was set at 15°, and the indices of placental blood perfusion were calculated using the volume histogram as shown in Figure 1 [4]. The indices were automatically calculated and expressed as dimensionless parameters: (1) vascularization index (VI), the ratio between the number of colored voxels and the total number of voxels. VI indicates the concentration of blood vessels in the placental segment; (2) flow index (FI), the ratio between the sum of the voxel velocities (scaled on a scale of 0–100) and the total number of colored voxels. FI provides information on placental blood flow; and (3) vascularization-flow index (VFI), which equals  $VI \times FI/100$ , namely, the ratio of the sum of voxel velocities (scaled on a scale of 0–100) to the total number of voxels in the sample.

### Statistical methods

SPSS version 27.0 for Windows (IBM Corp, Armonk, NY, USA) was utilized for all statistical analyses. The

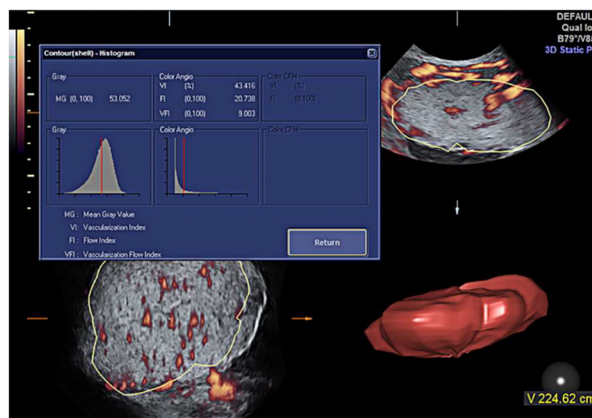


**Figure 1.** Placental blood flow measured by virtual organ computer-aided analysis software. Measures of blood flow obtained include the vascularization index (VI), flow index (FI), and vascular flow index (VFI).

normality of variable distribution was assessed using the Kolmogorov-Smirnov test. Continuous variables were compared using Student's t-test, while categorical variables were analyzed using the Chi-squared test. Receiver operating characteristic (ROC) curves were generated for each parameter to predict the diagnosis of FGR, and the area under the curve (AUC) was calculated to determine the sensitivity and specificity of each index for diagnosing FGR. When plotting the ROC curve of the combined blood flow indicator parameters, logistic regression was first employed to calculate the prediction probability, followed by the determination of the area, sensitivity, and specificity. Statistical significance was assessed two-sided at  $P$  value < 0.05.

### Results

A total of 73 pregnant patients with suspected FGR were recruited. 10 patients were excluded due to losing to follow-up ( $n=6$ ), missing data ( $n=4$ ), leaving 63 pregnancies available for analysis (Figure 2), which was divided into 31 cases of early-onset FGR (< 32 weeks) and 32 cases of late-onset FGR ( $\geq 32$  weeks). The study matched 115 uneventful pregnancies for gestational age with normal growth and healthy neonates, which were further divided into 57 cases and 58 cases, using 32 weeks as the boundary.

The characteristics of the 178 women between 20 and 40 weeks of gestation included in the study are presented in Table 1. Maternal age, GA at inclusion, and delivery mode did not show statistically significant differences between the study and control groups. The proportion of history of hypertension and diabetes was significantly higher in the late-onset FGR group when compared with control groups ( $P < 0.05$ ).

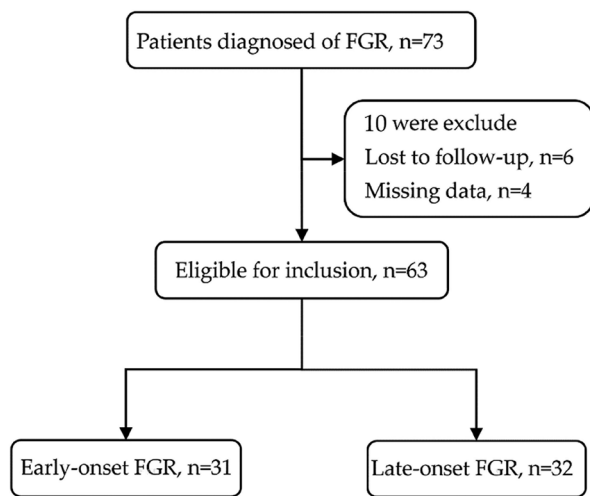


**Figure 2.** Process of pregnant patient inclusion. A total of 10 participants were excluded from the analyses because they were subsequently lost to follow-up, missing data. There were 63 eligible women enrolled. 31 pregnant women with early-onset FGR; the remaining 32 pregnant women with late-onset FGR.

Meanwhile, case groups delivered earlier, had neonates with lower birth weights, and had a higher incidence of composite adverse outcomes ( $P < 0.05$ ) than control groups. In the early-onset FGR group, 15 cases (women) were induced (51%), with a total of 12 neonates (75%) exhibiting composite adverse outcomes compared to 1 case (3%) and 17 neonates (54%) in the late-onset FGR group (Table 2).

Table 3 demonstrates that there were no significant differences between the two case groups in terms of maternal age, incidence of hypertension and anterior placenta, delivery mode, gender, and the interval difference between actual GA and ultrasonic GA ( $P > 0.05$ ). However, the incidence of diabetes in pregnant women and GA at delivery, neonate birth weight, and cesarean section rate were significantly lower in the early-onset FGR group, and the incidence of adverse neonatal outcomes was higher than those in the late-onset FGR group ( $P < 0.05$ ).

Significant differences between normal and FGR pregnancies were observed for all 2D or 3D Doppler measurement indices (Table 4). To determine whether blood indicators might serve as predictive markers of FGR, ROC curves (Table 5) were generated using all 2D or 3D Doppler measurement indices to compare discriminatory power for predicting FGR. In the early-onset FGR group, the diagnostic value of UA PI for predicting FGR was the highest, with an AUC of 0.861 (Figure 3). A UA PI of 1.315 was significantly associated with early-onset FGR, exhibiting 61.32% specificity and 94.71% sensitivity. When 2D parameter was combined,

**Table 1.** Demographic and obstetric characteristics of the study population.

Variable	<32 weeks				≥32 weeks			
	Case group (n=31)	Control group (n=57)	t/χ <sup>2</sup>	P value	Case group (n=32)	Control group (n=58)	t/χ <sup>2</sup>	P value
At inclusion								
Maternal age (years)	30.23 ± 5.80	28.40 ± 5.35	-1.48	0.142	29.16 ± 6.20	30.62 ± 4.83	1.242	0.218
Gestational age (weeks)	26.35 ± 3.38	26.77 ± 5.00	0.46	0.646	35.66 ± 2.51	35.88 ± 2.23	0.435	0.665
EFW (g) <sup>a</sup>	665.97 ± 314.88	1113.54 ± 496.67	4.54	<0.001	1866.78 ± 495.68	2640.64 ± 497.07	7.077	<0.001
Delivery								
Gestational age (weeks)	31.06 ± 2.84	38.61 ± 2.84	-3.45	0.004	37.38 ± 3.03	38.59 ± 3.09	-2.601	0.012
Neonate birth weight (g)	1399.97 ± 868.68	3249.40 ± 467.77	-11.017	<0.001	2204.38 ± 578.55	3330.26 ± 510.37	-9.550	<0.001
Fetal gender								
Female	19 (61.3%)	26 (45.6%)	1.390	0.237	25 (78.1%)	31 (53.4%)	5.340	0.021
Male	12 (38.7%)	31 (54.4%)			7 (21.9%)	27 (46.6%)		
Delivery mode								
Vaginal delivery	20 (64.5%)	27 (47.4%)	2.373	0.123	10 (31.3%)	27 (46.6%)	1.994	0.158
Cesarean section	11 (35.5%)	30 (52.6%)			22 (68.8%)	31 (53.4%)		

<sup>a</sup>Estimated fetal weight.

<sup>b</sup>Calculation is meaningless.

AUC was 0.922. When placental 3D vascular indices were used as joint diagnostic indices, the AUC was 0.921, which did not improve diagnostic accuracy. The AUC of CPR in the late-onset FGR group was 0.874 (Figure 4). When the placental blood perfusion indices were used as joint diagnostic indices, the AUC was 0.957, which demonstrated the highest diagnostic value for predicting late-onset FGR, with 83.95% specificity, 98.32% sensitivity, and a Youden index of 0.821 when a prediction probability of < 0.552 was applied as the positive cutoff value.

The positive and negative likelihood ratios were shown in Table 5. In the early-onset FGR group, the positive likelihood ratio (PLR) of CPR (4.578) was the largest among the 2D Doppler indices, and the PLR increased significantly after the combination of 2D indices (21.938), which has the highest efficiency of true positive prediction. Among the 3D Doppler indices, the PLR of VI (14.250) is the largest, which is still lower than that of the 2D joint indicators. The combination of 2D and 3D Doppler indices (4,620) did not improve the efficiency of true positive prediction. In the late-onset FGR group, the PLR of CPR (2.991) was the largest among the 2D Doppler indices, and the combination of 2D Doppler indices (3.096) did not

significantly improve the efficiency of true positive prediction. Among the 3D Doppler indices, the PLR of FI (7.825) was the highest, and the PLR was further increased after combining the 3D indices (8.536), which has the highest efficiency of true positive prediction.

In the early-onset FGR group, the negative likelihood ratio (NLR) of CPR (0.313) is the highest among the 2D Doppler parameters, while VFI (0.565) is the highest among the 3D Doppler parameters. The NLR of UA SD (0.349) in the late-onset FGR group is the highest among the 2D Doppler parameters, while VFI (0.557) is the highest among the 3D Doppler parameters. The combination of 2D indicators (0.308,0) and 3D indicators (0.464, 0.02) in the early and late onset FGR groups did not improve the efficiency of true negative prediction.

## Discussion

FGR is commonly defined as the failure of a fetus to achieve its genetic growth potential. The two primary phenotypes of FGR, early-onset and late-onset FGR, differ in various aspects, with an incidence of FGR in China reported at 6.39% [6]. Fetal size is determined by BPD, HC, AC, FL, and/or EFW, which are calculated using different formulas. Consequently, fetal growth assessment cannot rely solely on the biometric measurement of fetal size.

In order to diagnose FGR as early as possible and enhance pregnancy outcomes, it is essential to establish examination indices that can predict the growth and development of the fetus in utero. This study aims to analyze differences in arterial 2D Doppler and 3D placental blood perfusion indices, explore the application value of ultrasound for hemodynamic changes in FGR, and identify valuable parameter indices. Regarding the measurement of blood flow data, some studies [7]

**Table 2.** Neonatal outcomes.

Variable	Case group	
	Early-onset (n=31)	Late-onset (n=32)
Induction of labor	15 (48.38%)	1 (3.12%)
Adverse neonatal outcomes <sup>a</sup>	12 (75.00%)	17 (54.83%)
Premature birth	9	8
Neonatal death	1	1
NRDS <sup>b</sup>	5	1
Apgar score at 1-min < 7	1	0
LBWI <sup>c</sup>	12	17

Data are presented as number (%).

<sup>a</sup>Multiple conditions possible; described in live birth fetuses.

<sup>b</sup>NRDS, neonatal respiratory distress syndrome.

<sup>c</sup>LBWI, Low birth weight infant.

**Table 3.** General information between early- and late-onset FGR.

Variable	Case group			<i>t</i> / $\chi^2$	<i>P</i> value
	Early-onset (n=31)	Late-onset (n=32)			
Maternal age (years)	30.23 ± 5.80	29.16 ± 6.20		0.928	0.357
History of hypertension	6 (19.35%)	5 (15.63%)		3.421	0.266
History of diabetes	0 (0%)	4 (12.50%)		-2.440	0.015
Anterior placenta	15 (48.38%)	13 (40.63%)		2.874	0.541
Interval difference (days) <sup>a</sup>	20.16 ± 10.98	24.03 ± 7.94		-1.610	0.113
Gestational age at delivery (weeks)	31.06 ± 2.84	37.38 ± 3.03		-6.250	< 0.001
Neonate birth weight (g)	1399.97 ± 868.68	2204.38 ± 578.55		-4.312	< 0.001
Adverse pregnancy outcomes	24 (77.42%)	10 (31.25%)		13.511	< 0.001
Gender					
Female	19 (61.29%)	25 (78.12%)		2.119	0.146
Male	12 (38.7%)	7 (21.9%)			
Delivery mode					
Vaginal delivery	20 (64.5%)	10 (31.3%)		6.986	0.008
Cesarean section	11 (35.5%)	22 (68.8%)			

<sup>a</sup>The difference between the actual diagnosis gestational week and the gestational week measured by ultrasound.

**Table 4.** Blood flow-related parameters of subjects with <32 weeks and ≥32 weeks.

Blood flow index	<32 weeks				≥32 weeks			
	Case group (n=31)	Control group (n=57)	t	P value	Case group (n=32)	Control group (n=58)	t	P value
<b>2D</b>								
UA S/D	5.78±3.54	2.90±0.70	-4.481	< 0.001	3.28±1.01	2.35±0.37	-5.036	< 0.001
UA PI	1.55±0.51	0.99±0.21	-5.906	< 0.001	0.67±0.09	0.58±0.11	-4.160	< 0.001
UA RI	0.77±0.10	0.67±0.28	-2.487	0.021	1.09±0.25	0.82±0.16	-6.127	< 0.001
MCA S/D	4.17±1.20	5.25±1.58	3.292	< 0.001	3.89±1.18	4.82±1.26	3.407	0.001
MCA PI	1.43±0.32	1.72±0.26	4.665	< 0.001	1.36±0.33	1.66±0.27	4.745	< 0.001
MCA RI	0.74±0.08	0.79±0.11	2.429	0.025	0.73±0.08	0.79±0.05	3.894	< 0.001
CPR	1.06±0.58	1.84±0.56	6.163	< 0.001	1.33±0.49	2.11±0.53	6.820	< 0.001
UTA S/D	3.31±1.24	2.16±0.63	-4.828	< 0.001	2.32±0.77	2.00±0.30	-2.292	0.028
UTA PI	1.38±0.55	0.83±0.28	-5.263	< 0.001	0.88±0.29	0.74±0.17	-2.941	0.004
UTA RI	0.65±0.13	0.51±0.09	-5.614	< 0.001	0.54±0.10	0.49±0.07	-2.385	0.019
<b>3D</b>								
VI	11.53±7.49	21.01±11.77	4.053	< 0.001	14.12±7.17	18.42±8.97	2.328	0.022
FI	31.83±9.68	40.75±14.17	3.139	< 0.001	35.00±7.09	48.68±10.60	6.531	< 0.001
VFI	4.83±4.92	8.97±6.04	3.266	< 0.001	5.41±3.13	9.12±5.37	3.586	0.001

Abbreviations. S/D, systolic/diastolic velocity ratio; PI, pulsatility index; RI, resistance index; UA, umbilical artery; MCA, middle cerebral artery; CPR, cerebroplacental ratio (the ratio of MCA PI to UA PI); UTA, uterine artery; VI, vascular index; FI, flow index; VFI, vascular flow index.

**Table 5.** ROC Curve results of the fetal parameters of FGR.

Test result variable	Early-onset						Late-onset							
	AUC	Positive cutoff value	Sensitivity	Specificity	Youden's index	PLR	NLR	AUC	Positive cutoff value	Sensitivity	Specificity	Youden's index	PLR	NLR
<b>2D</b>														
UA SD	0.817	4.698	0.982	0.548	0.531	2.173	0.033	0.802	2.545	0.741	0.742	0.483	2.872	0.349
UA PI	0.861	1.315	0.947	0.613	0.560	2.447	0.086	0.811	1.095	0.983	0.516	0.499	2.031	0.033
UA RI	0.820	0.780	0.965	0.548	0.513	2.135	0.064	0.786	0.679	0.966	0.484	0.449	1.872	0.070
MCA SD	0.686	3.735	0.930	0.452	0.381	1.697	0.155	0.741	3.815	0.828	0.645	0.473	2.332	0.267
MCA PI	0.748	1.505	0.789	0.677	0.467	2.443	0.312	0.630	1.425	0.862	0.677	0.539	2.669	0.204
MCA RI	0.686	0.735	0.895	0.452	0.346	1.633	0.232	0.610	0.735	0.828	0.645	0.473	2.332	0.267
CPR	0.856	1.391	0.737	0.839	0.576	4.578	0.313	0.874	1.457	0.966	0.677	0.643	2.991	0.050
UTA SD	0.796	2.704	0.895	0.677	0.572	2.771	0.155	0.612	2.530	0.948	0.290	0.239	1.335	0.179
UTA PI	0.793	1.219	0.930	0.645	0.575	2.620	0.109	0.630	1.010	0.966	0.323	0.288	1.427	0.105
UTA RI	0.774	0.645	0.947	0.581	0.528	2.260	0.091	0.610	0.605	0.931	0.290	0.221	1.311	0.238
2D combined	0.922	0.858	0.702	0.968	0.669	21.938	0.308	0.909	0.373	1.000	0.677	0.677	3.096	0.000
<b>3D</b>														
VI	0.748	22.690	0.456	0.968	0.424	14.250	0.562	0.629	6.005	1.000	0.258	0.258	1.348	0.000
FI	0.683	40.335	0.561	0.871	0.432	4.349	0.504	0.862	42.500	0.759	0.903	0.662	7.825	0.267
VFI	0.732	7.424	0.526	0.839	0.365	3.267	0.565	0.712	7.610	0.569	0.774	0.343	2.518	0.557
3D combined	0.787	0.729	0.596	0.871	0.467	4.620	0.464	0.878	0.665	0.828	0.903	0.731	8.536	0.190
<b>2D+3D</b>														
2D combined + 3D combined	0.921	0.332	0.982	0.742	0.724	3.806	0.024	0.957	0.552	0.983	0.839	0.821	6.106	0.02

Abbreviations. S/D, systolic/diastolic velocity ratio; PI, pulsatility index; RI, resistance index; UA, umbilical artery; MCA, middle cerebral artery; CPR, cerebroplacental ratio (the ratio of MCA PI to UA PI); UTA, uterine artery; VI, vascular index; FI, flow index; VFI, vascular flow index; PLR, positive likelihood ratios; NLR, negative likelihood ratios.

have demonstrated that repeated measurements do not predict outcome and prognosis results for FGR more effectively than the initial measurement; thus, this study utilizes only the first measurement data at inclusion.

### Ultrasonic detection of fetal arterial blood flow

During a normal pregnancy, as GA increases, the fetal UA, MCA, and maternal UtA gradually mature. The vascular diameter progressively thickens, and the blood flow resistance between the mother and fetus

continuously decreases. However, placental vascular resistance rises in cases with FGR [8]. In this study, the UA PI in case groups was higher than that in control groups, suggesting that blood flow resistance had increased, and placental perfusion was impaired.

The fetal MCA is a crucial artery supplying fetal intracranial nutrition. Under anoxic conditions, fetal blood redistributes by increasing blood flow to the brain, heart, and adrenal glands while reducing blood flow to the peripheral circulation. This blood redistribution is called the brain-sparing effect, characterized by an increase in the end-diastolic velocity of blood flow in the MCA

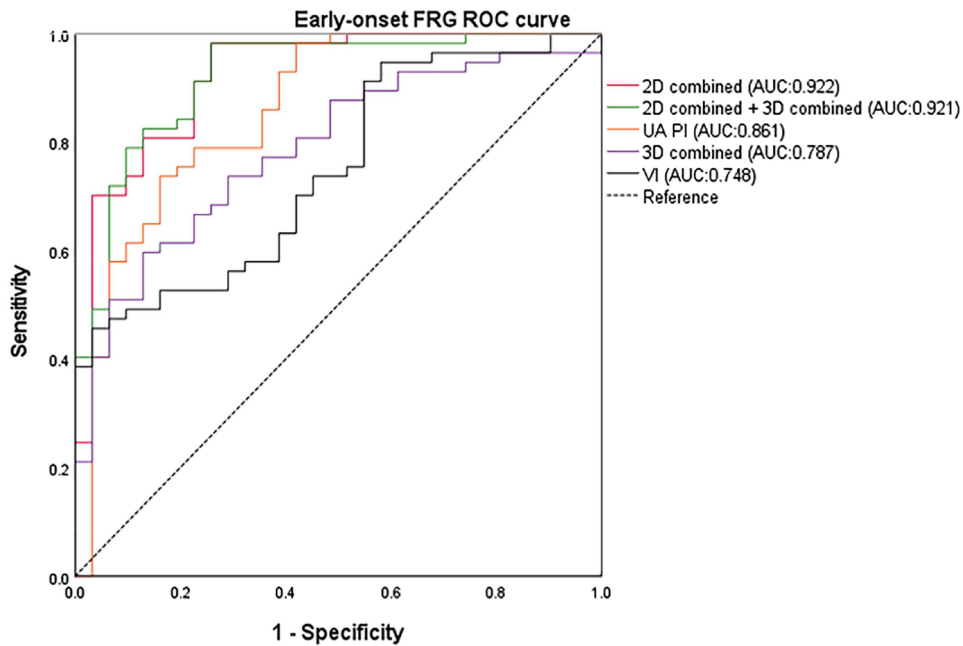


**Figure 3.** Roc curve of Early-onset FGR. For early-onset FGR, the diagnostic efficacy was highest in the 2D parameter with the largest UA PI AUC (0.861), increased in AUC (0.922) when the 2D parameter was combined, and did not increase when the 2D parameter was combined with the 3D parameter.

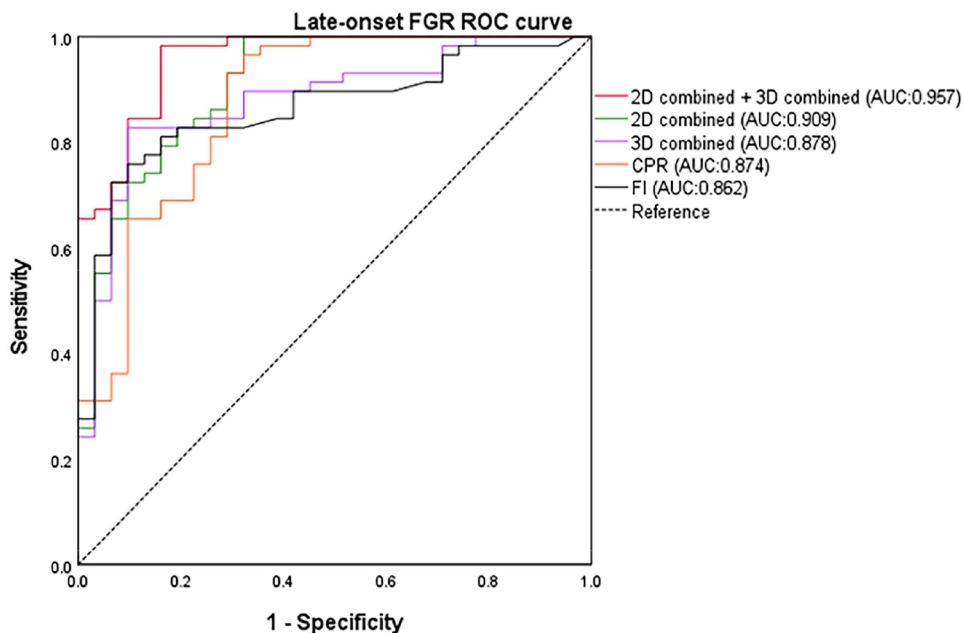


**Figure 4.** Roc curve of Late-onset FGR. For late-onset FGR, the diagnostic efficacy was highest with the largest CPR AUC (0.874) among the 2D parameters, increased (AUC 0.909) when the 2D parameters were combined, and significantly increased (0.957) when the 2D parameters were combined with the 3D parameters.

on the Doppler spectrum [9]. In this study, compared to the control group, the indices of the MCA blood flow spectrum of fetuses in the early- and late-onset FGR groups were significantly lower, indicating that fetuses in the FGR groups may have experienced chronic intrauterine hypoxia, resulting in blood redistribution in vivo.

The calculation of the CPR, the ratio of MCA to UA PI, eliminates the influence of cardinal fluctuations and interference of common external factors, thereby reducing error. The PI of the MCA is always higher than that of the UA in normal pregnancy, and CPR is consistently greater than 1 [10]. When fetal intrauterine hypoxia

occurs, the monitoring indices of UA blood flow increase, those of MCA blood flow decrease, and CPR declines. In this study, the CPR in both the early- and late-onset FGR groups was lower than that in the control group, suggesting the fetus had developed intrauterine chronic hypoxia.

Uterine arterial hemodynamics reflect uterine and placental circulation. As pregnancy progresses, the resistance of UtA blood flow in women with a normal pregnancy significantly decreases [11]. The increased UtA PI and the presence of early diastolic traces in late pregnancy women confirm abnormal uterine placental circulation during pregnancy [12]. This study found that the UtA index of both the early- and late-onset FGR groups was higher than that of the control group ( $p < 0.05$ ), indicating increased uterine placental perfusion resistance in the FGR group.

### **Detection of placental blood perfusion**

Factors affecting fetal growth and development in utero primarily include maternal, fetal, and umbilical cord placental factors, with placental factors being the most crucial [13]. Uterine placental blood flow in pregnant women with FGR is over 50% lower than that in normal pregnant women [6]. Prior research has demonstrated that Power Doppler ultrasonography outperforms CDFI in assessing low-speed blood flow, and 3D power Doppler ultrasound can evaluate the overall blood flow of a tissue or organ. This technique can not only express tissue vascular density and display the 3D spatial relationship between vascular shape and branches but also provide indirect blood cell volume per unit volume data [14]. In this study, the VI, FI, and VFI of the early- and late-onset FGR groups were lower than those of the control groups, suggesting higher placental resistance and significantly lower placental blood perfusion in the FGR group compared to the control group. The placental blood perfusion indexes of VI, FI, and VFI increased with the increase in GA, indicating that the vascular network and blood flow in the placenta also increased with the rise in GA. Chen et al. [15] recently published notable findings that VI and VFI were valuable for predicting FGR at the 32–36<sup>+6</sup> weeks stage, consistent with our assertion that 3D power Doppler ultrasound was valuable for predicting late-onset FGR.

Due to differences in placental pathological bases, index changes varied between early- and late-onset FGR. Early-onset FGR was primarily caused by poor placental implantation, abnormal spiral arteries, and maternal vascular malnutrition, resulting in UA PI

preceding other Doppler changes. This study found that sensitivity and specificity of UA PI were highest in the early-onset FGR group. In those with late-onset FGR, the placenta did not exhibit specific changes, as alterations are mostly diffuse. Our data reveals that UA appears to be a good predictor of early-onset FGR due to its high sensitivity levels; conversely, the prediction models for late-onset FGR developed using combined blood flow indices outperformed those devised using 2D measurements, with AUC values of 87%. It is suggested that placental function be monitored more closely when the combined placental 3D power Doppler index is lower than 0.33 at 32–36<sup>+6</sup> weeks gestation, even if blood flow parameters of the UA, MCA, and UtA are normal, to facilitate early FGR detection and improve perinatal prognosis.

Early-onset FGR occurs less frequently but presents more severe clinical manifestations than late-onset FGR, such as earlier GA at delivery, increased risk of neonatal admission to the NICU, and more induced prematurity [16]. They are often associated with hypertensive disorders of pregnancy. In this study, 16 cases were induced, among which 15 had early-onset FGR, displaying significantly lower neonate birth weights than the late-onset FGR group. One fetus in the early-onset FGR group was first diagnosed at 31<sup>+6</sup> weeks but appeared to be 21<sup>+5</sup> weeks by ultrasound. The pregnant woman was immediately hospitalized and gave birth to a healthy girl. Therefore, timely detection and adequate identification of FGR can provide a basis and reference for developing effective clinical intervention measures.

Of course, our research also has limitations. That patients who have lost follow-up and have no result data are excluded leads to insufficient case number, and it is not known whether the prognosis of these patients is good or bad, and we were not able to evaluate both short- and long-term neurodevelopmental dysfunction, which may be more related to aberrations in cerebral blood flow than the short-term neonatal outcomes evaluated in this study.

### **Conclusion**

3D power Doppler measurement of placental blood flow is significantly altered in FGR. Moreover, this measurement, combined with 2D Doppler, demonstrated superior predictive value for diagnosing late-onset FGR compared to other conventional indicators. Compared with 2D Doppler indicators, the 3D power index, VFI, has a good true-negative predictive value for both early- and late-onset FGR.

## Acknowledgments

The authors are grateful to the women whose data has made this work possible and the funding support.

## Authors' contributions

Research design, Changfu Hao and Hui Fan; Conducted the experiments, Hui Fan; Performed the data analysis, Changfu Hao and Lili Li; Wrote or contributed to the writing of the manuscript, Hui Fan and Lili Li; Funding acquisition, Changfu Hao. Hui Fan, Lili Li and Changfu Hao have equal contribution to the present work. All authors have read and agreed to the published version of the manuscript.

## Ethics statement

The study protocol conformed to the ethical guidelines of the 1975 Declaration of Helsinki and was approved by the Ethics Committee of the Third Affiliated Hospital of Zhengzhou University (Approval Number: 2020-094). Informed consent was obtained from all subjects involved in the study.

## Disclosure statement

No potential conflict of interest was reported by the author(s).

## Funding

This research was funded by National Natural Science Foundation of China (No. 82173491).

## ORCID

Lili Li  <http://orcid.org/0000-0002-4458-2634>

## Data availability statement

Data will be available upon request.

## References

- [1] Roeckner JT, Pressman K, Odibo L, et al. Outcome-based comparison of SMFM and ISUOG definitions of fetal growth restriction. *Ultrasound Obstet Gynecol.* 2021;57(6):1–9. doi: [10.1002/uog.23638](https://doi.org/10.1002/uog.23638).
- [2] Martins JG, Biggio JR, Abuhamad A, Society for maternal-fetal medicine consult series #52: diagnosis and management of fetal growth restriction: (replaces clinical guideline number 3, april 2012). *Am J Obstet Gynecol.* 2020;223(4):B2–b17. doi: [10.1016/j.ajog.2020.05.010](https://doi.org/10.1016/j.ajog.2020.05.010).
- [3] Oros D, Figueras F, Cruz-Martinez R, et al. Longitudinal changes in uterine, umbilical and fetal cerebral Doppler indices in late-onset small-for-gestational age fetuses. *Ultrasound Obstet Gynecol.* 2011;37(2):191–195. doi: [10.1002/uog.7738](https://doi.org/10.1002/uog.7738).
- [4] Yamasato K, Zalud I. Three dimensional power Doppler of the placenta and its clinical applications. *J Perinat Med.* 2017;45(6):693–700. doi: [10.1515/jpm-2016-0366](https://doi.org/10.1515/jpm-2016-0366).
- [5] Hong-Bo LX-fQ. Placental factor and clinical diagnosis and treatment of fetal growth restriction. *Chin J Pract Gynecol Obstet.* 2016;32(04):298–302.
- [6] Lees C, Stampalija T, Baschat AA, et al. ISUOG practice guidelines: diagnosis and management of small-for-gestational-age fetus and fetal growth restriction. *Ultrasound Obstet Gynecol.* 2020;56(2):298–312. doi: [10.1002/uog.22134](https://doi.org/10.1002/uog.22134).
- [7] Mylrea-Foley B, Wolf H, Stampalija T, et al. Longitudinal Doppler assessments in late preterm fetal growth restriction. *Ultraschall Med.* 2021;44(1):56–67. doi: [10.1055/a-1511-8293](https://doi.org/10.1055/a-1511-8293).
- [8] Burton GJ, Jauniaux E. Pathophysiology of placental-derived fetal growth restriction. *Am J Obstet Gynecol.* 2018;218(2s):S745–s761. doi: [10.1016/j.ajog.2017.11.577](https://doi.org/10.1016/j.ajog.2017.11.577).
- [9] Rizzo G, Mappa I, Bitsadze V, et al. Role of Doppler ultrasound at time of diagnosis of late-onset fetal growth restriction in predicting adverse perinatal outcome: prospective cohort study. *Ultrasound Obstet Gynecol.* 2020;55(6):793–798. doi: [10.1002/uog.20406](https://doi.org/10.1002/uog.20406).
- [10] Ciobanu A, Wright A, Syngelaki A, et al. Fetal medicine foundation reference ranges for umbilical artery and Middle cerebral artery pulsatility index and cerebroplacental ratio. *Ultrasound Obstet Gynecol.* 2019;53(4):465–472. doi: [10.1002/uog.20157](https://doi.org/10.1002/uog.20157).
- [11] Hawkes RA, Patterson AJ, Priest AN, et al. Uterine artery pulsatility and resistivity indices in pregnancy: comparison of MRI and Doppler US. *Placenta.* 2016;43:35–40. doi: [10.1016/j.placenta.2016.04.002](https://doi.org/10.1016/j.placenta.2016.04.002).
- [12] Ghosh GS, Gudmundsson S. Uterine and umbilical artery Doppler are comparable in predicting perinatal outcome of growth-restricted fetuses. *BJOG.* 2009;116(3):424–430. doi: [10.1111/j.1471-0528.2008.02057.x](https://doi.org/10.1111/j.1471-0528.2008.02057.x).
- [13] Wang LQ, Fernandez-Boyano I, Robinson WP. Genetic variation in placental insufficiency: what have we learned over time? *Front Cell Dev Biol.* 2022;10:1038358. doi: [10.3389/fcell.2022.1038358](https://doi.org/10.3389/fcell.2022.1038358).
- [14] Hata T, Tanaka H, Noguchi J, et al. Three-dimensional ultrasound evaluation of the placenta. *Placenta.* 2011;32(2):105–115. doi: [10.1016/j.placenta.2010.11.001](https://doi.org/10.1016/j.placenta.2010.11.001).
- [15] Chen JY, Chen M, Wu XJ, et al. The value of placental vascularization indices for predicting preeclampsia and fetal growth restriction in different stages of gestation: a prospective and longitudinal study. *Placenta.* 2022;122:1–8. doi: [10.1016/j.placenta.2022.03.124](https://doi.org/10.1016/j.placenta.2022.03.124).
- [16] Gordijn SJ, Beune IM, Ganzevoort W. Building consensus and standards in fetal growth restriction studies. *Best Pract Res Clin Obstet Gynaecol.* 2018;49:117–126. doi: [10.1016/j.bpobgyn.2018.02.002](https://doi.org/10.1016/j.bpobgyn.2018.02.002).